Journal of Electrical Engineering, Jee, no.2, volume 17, 2017, pp. 413-421.

Improvement of Microgrid (MG) Systems Using Synchronverters (SVs)

Mohammad A. elsayad [1], Amr M. Abdin [1], Mohamed H. Shaalan [2]
[1]Elect. Power &Machine Dept., Faculty of Eng. Ain-Shames University, Cairo, Egypt
[2]Elect. Eng. Dept., Benha Faculty of Engineering, Benha University, Qalubiya, Egypt
e-mail: Mohamed.shaalan@bhit.bu.edu.eg

***Abstract*- In this paper, the synchronverter (SV) model is revised and thoroughly examined. Detailed simulation blocks are clarified and presented using Matlab/Simulink. The aim is to enhance inertia contribution to approach equivalent real synchronous generator (SG) and by another meaning grid-friendly inverter that mimic the operation of conventional SG. Improvements in the two modes of operation grid-connected mode and stand-alone mode are obtained. SV is able to transfer seamlessly between the two modes and hence, they provide an ideal solution for smart grids and microgrids (MGs). An automatic synchronization unit is used to minimize disturbances at instant of connection to grid. Unlike most previous works in this area of research, the present one simulates also the pulse width modulation (PWM) inverter to monitor the dc bus condition during different conditions of operation. Simulation results are presented to verify all the above ideas.**

***Index Terms*- Distributed generation (DG), frequency drooping, load sharing, microgrid (MG), parallel inverters, pulse width modulation (PWM) inverter, renewable energy (RE), smart grid, synchronous generator (SG), static synchronous generator (SSG), synchronverter (SV), virtual synchronous generator (VSG), voltage drooping.**

I. INTRODUCTION

The share of electrical energy produced by renewable-energy sources (RESs), such as wind power and solar power… etc., is gradually increasing. Comparing with conventional power stations RESs are distributed in nature, so they are usually called distributed generators (DG).The electrical authority in Egypt planned to cover 20% of bulk energy generation by RESs by 2020 as an attempt to solve the electricity crisis. And in European countries, the USA, China, and India significant targets are also aimed for using the DGs and RESs in their power systems up to next two decades. Worldwide, the electrical power system is currently undergoing a dramatic change from centralized generation to distributed generation. Most of this DG needs dc–ac conversion, to interface with the public-utility grid. For example, wind turbines are most effective if free to generate at variable frequency, so they require double conversion ac–dc–ac while photovoltaic arrays require a single dc–ac conversion. This means that more and more inverters will be connected to the grid and will eventually dominate power generation.

The current paradigm in the control of RESs is to extract the maximum power from the power source and inject them all into the power grid [1] Advanced algorithms have been developed to ensure that the current injected into the grid is clean sinusoidal [2], [3]. The policy of injecting all available power to the grid is a good one as long as renewable power sources constitute a small part of the grid power capacity. Indeed, any random power fluctuation of the renewable power generators will be compensated by the controllers associated with the large conventional generators, and some of these generators will also take care of the overall power balance, system stability, and fault ride through [4],[5].

When renewable power generators will provide the majority of the grid power, the need will arise to operate them in the same way as conventional power generators or at least to imitate certain aspects of the operation of conventional generators using novel techniques [6]. This will require high-efficiency energy-storage units so that the random fluctuations of the prime power source can be filtered out [7] – [14]. The key problem here is how to control the inverters in DGs so that these inverters can be integrated into the existing system and behave in the same way as conventional SG does. This assures a smooth transition from the existing conventional power grid to a grid dominated by inverters.

In paper [4], a method by which an inverter can be operated to mimic the behavior of an SG is proposed. The dynamic equations are the same; only the mechanical power exchanged with the prime mover is replaced with the power exchanged with the dc bus. The inverter including the filter inductors, capacitors and the associated controller is called a SV. A SV will have all the properties of a SG, which is a complex nonlinear system. The parameters, such as inertia, friction coefficient, field inductance, and mutual inductances can be selected without criteria of real material limitations present in SGs. The energy that would be lost in the virtual mechanical friction is not lost in reality; it is directed back to the dc bus. Moreover, no magnetic saturation and no eddy currents are present in this case. Parameter values that are impossible in a real SG and variation of parameters while the system is operating are benefits in this case.

If a SV is connected to the utility grid and is operated as a generator, no difference would be felt from the grid side between this system and an SG. Thus, the conventional control algorithms and equipment that have been developed for SGs driven by prime movers can be applied to SVs [4].

IEEE has defined a term, called static synchronous generator (SSG) [15], to designate a static switching power converter supplied from an appropriate electric energy source and operated to produce a set of adjustable multiphase output voltages, which may be coupled to an ac power system for the purpose of exchanging independently controllable real and reactive power in flexible ac transmission system. Clearly, SVs is a particular type of SSGs.

The concept of a virtual synchronous machine (VISMA) was proposed in [10], [11], [14]-[19], where the voltages at the point of common coupling with the grid are measured to calculate the phase currents of the VISMA in real time. These currents are then used as reference currents for the inverter, and hence, the inverter behaves as a current source connected to the grid. If the current tracking error is small, then the inverter behaves like a synchronous machine, justifying the term VISMA. If the current tracking error is large, then the inverter behaviors change. As a key difference to the SV, it is

worth mentioning that the SV does not depend on the tracking of reference currents or voltages.

In [16], a short-term energy-storage system is added to the inverter in order to provide virtual inertia to the system. The power flow to the storage is proportional to the derivative of the grid frequency (as it would be with real inertia). This kind of inverter with added virtual inertia, called virtual synchronous generators (VSGs), can contribute to the short-term stabilization of the grid frequency. However, the system dynamics seen from the grid side will be different from those of a SG.

The rest of this paper is organized as follows. In Section II, a dynamic model of SGs is established. The way to simulate performance of a SV is described in Section III, and issues related to its operation, e.g., frequency- and voltage-drooping mechanisms for load sharing, are described in Section IV. Simulation results are given in Section V with conclusions in Section VI.

II. MODELING SYNCHRONOUS MACHINES

The model of synchronous machines can be found in many sources such as [3], [4], [20]–[27]. Here, the model established in [4] is used. It considers the following assumptions:

- Rotor type: round rotor machine so that all stator inductances are constant.
- The effect of damper windings in the rotor is neglected.
- There is one pair of poles.
- There are no magnetic-saturation effects in the iron core and no eddy currents.

That paper uses relatively very small inertia so simulation and experimental results seem to have negligible hunting (oscillations around the synchronous frequency), and shows exceptionally fast synchronization. In present work trying to have similar response at practical values of inertia necessitates using high values of drooping frequency coefficient as will be shown in IV.

A. Electrical Part

The field and the three identical stator windings are distributed in slots around the periphery of the uniform air gap. The stator windings can be regarded as concentrated coils having self-inductance L and mutual inductance –M (M >0 with a typical value 1/2L, the negative sign is due to the 2π/3 phase angle), as shown in Fig. 1. The field (or rotor) winding can be regarded as a concentrated coil having self-inductance L_f. The mutual inductance between the field coil and each of the three stator coils varies with the rotor angle θ, i.e.,

$$M_{af} = M_f \cos(\theta)$$

$$M_{bf} = M_f \cos(\theta - \frac{2\pi}{3})$$

$$M_{cf} = M_f \cos(\theta - \frac{4\pi}{3})$$

Where $M_f > 0$, the flux linkages of the windings are

$$\Phi_a = Li_a - Mi_b - Mi_c + M_{af}\, i_f$$

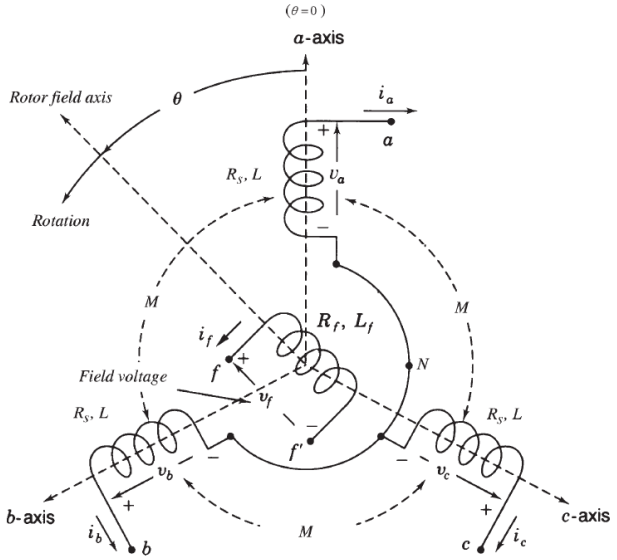

Fig.1. Structure of an idealized three-phase round-rotor SG modified from [4], [20].

$$\Phi_b = -Mi_a + Li_b - Mi_c + M_{bf}\, i_f$$

$$\Phi_c = -Mi_a - Mi_b + Li_c + M_{cf}\, i_f$$

$$\Phi_f = M_{af}\, i_a + M_{bf}\, i_b + M_{cf}\, i_c + L_f i_f$$

Where i_a, i_b and i_c are the stator phase currents and i_f is the rotor excitation current. Denote

$$\Phi = \begin{bmatrix}\Phi_a \\ \Phi_b \\ \Phi_c\end{bmatrix} \quad , \quad i = \begin{bmatrix} i_a \\ i_b \\ i_c\end{bmatrix}$$

$$\widetilde{cos}\,\theta = \begin{bmatrix} \cos\theta \\ \cos(\theta - \frac{2\pi}{3}) \\ \cos(\theta - \frac{4\pi}{3})\end{bmatrix}, \widetilde{sin}\,\theta = \begin{bmatrix} \sin\theta \\ \sin(\theta - \frac{2\pi}{3}) \\ \sin(\theta - \frac{4\pi}{3})\end{bmatrix}$$

Assume for the moment that the neutral line is not connected, then

$$i_a + i_b + ic = 0$$

It follows that the stator flux linkages can be rewritten as

$$\Phi = L_s i + M_f\, i_f\, \widetilde{cos}\,\theta \qquad (1)$$

Where $L_s = L + M$, and the field flux linkage can be rewritten as

$$\Phi_f = L_f\, i_f + M_f \langle i, \widetilde{cos}\,\theta \rangle \qquad (2)$$

Where $\langle \cdot,\cdot \rangle$ denotes the conventional inner product in $\mathbf{R}^3$. The second term $M_f \langle i, \widetilde{cos}\,\theta \rangle$ (called armature reaction) is constant if the three phase currents are sinusoidal (as functions of θ) and balanced. Also $\sqrt{2/3}\,\langle i, \widetilde{cos}\,\theta \rangle$ is called the *d*-axis component of the current.

Assume that the resistance of the stator windings is R_s; then, the phase terminal voltages $v = [v_a\, v_b\, v_c]^T$ can be obtained from Eq. 1 as

$$v = -R_s\, i - d\Phi/dt = -R_s\, i - L_s\, di/dt + e \qquad (3)$$

Where $e = [e_a\ e_b\ e_c]^T$ is the back electromotive force (EMF) due to the rotor movement given by

$$e = M_f\ i_f\ \theta^{\cdot}\ \widetilde{sin}\ \theta - M_f\ di_f/dt\ \widetilde{cos}\ \theta \quad (4)$$

The voltage vector e is also called no-load voltage or synchronous internal voltage.

The field terminal voltage is

$$v_f = -R_f\ i_f - d\Phi_f/dt \quad (5)$$

Where R_f is the resistance of the rotor winding. This completes the modeling of the electrical part of the machine.

B. Mechanical Part

The mechanical part of the machine is governed by

$$J\ \theta^{\cdot\cdot} = T_m - T_e - D_p\ \theta^{\cdot} \quad (6)$$

Where J is the moment of inertia of all the parts rotating with the rotor, T_m is the mechanical torque, T_e is the electromagnetic toque, and D_p is a damping factor. T_e can be found from the energy E stored in the machine magnetic field, i.e.,

$$E = \tfrac{1}{2}\langle i, \Phi\rangle + \tfrac{1}{2}\, i_f \Phi_f = 1/2\langle i, Lsi + M_f i_f\ \widetilde{cos}\ \theta\rangle + 1/2 i_f\ (L_f\ i_f + M_f\ \langle i, \widetilde{cos}\theta\rangle) = 1/2\langle i, L_s i\rangle + M_f\ i_f\ \langle i, \widetilde{cos}\ \theta\rangle + 1/2 Lf\ if^2$$

From simple energy considerations [20] we have

$$T_e = \partial E/\ \partial\theta\ |_{\Phi, \Phi_f\ constant}$$

Because constant flux linkages mean no back EMF, all the power flow is mechanical. It is not difficult to verify (using the formula for the derivative of the inverse of a matrix function) that this is equivalent to

$$T_e = -\ \partial E/\ \partial\theta\ |_{i, i_f\ constant}$$

Thus

$$T_e = -\ M_f\ i_f\ \langle i, \partial/\ \partial\theta\ \widetilde{cos}\ \theta\rangle = M_f\ \ i_f\ \langle i, \widetilde{sin}\ \theta\rangle \quad (7)$$

We mention that $\sqrt{2/3}\langle i,\ \widetilde{sin}\theta\rangle$ is called the q-axis component of the current. Note that if $i = i_0\ \widetilde{sin}\phi$ for some arbitrary angle ϕ, then

$$T_e = M_f i_f\ i_0 \langle \widetilde{sin}\theta, \widetilde{sin}\phi\rangle = 3/2\ M_f i_f\ i_0\ \widetilde{cos}(\theta - \phi)$$

Note also that if i_f is constant (as is usually the case), then Eq. 7 with Eq. 4 yields

$$T_e\theta^{\cdot} = \langle i, e\rangle$$

III. IMPLEMENTATION OF SYNCHRONVERTER

In this section, the details on how to implement a SV will be described. A simple dc/ac converter (inverter) used to convert dc power into three-phase ac is shown in Fig. 2. It includes three inverter legs operated using pulse width modulation (PWM) and *LC* filters to reduce the voltage ripple (and hence, the current ripple) caused by the switching.

In grid-connected operation, the impedance of the grid should be included in the impedance of the inductors L_g (with series resistance R_g), and then we may consider that after the circuit breaker, we have an infinite bus.

The *power part of the SV* is the circuit to the left of the three capacitors, together with the capacitors. If we disregard the ripple, then this part of the circuit will behave like an SG connected in parallel with the same capacitors. The inductors, denoted as L_g, are not part of the SV, but it is useful to have them (for synchronization and power control). It is important to have some energy storage (not shown) on the dc bus (at the left end of the figure) since the power absorbed from the dc bus represents not only the power taken from the imaginary prime mover but also from the inertia of the rotating part of the imaginary SG. This latter component of the power may come in strong bursts, which is proportional to the derivative of the grid frequency.

Block diagram in Fig. 3. These two parts interact via the signals e and i (v and v_g will be used for controlling the SV).

A. Power Part

The terminal voltages $v = [v_a\ v_b\ v_c]^T$ of the imaginary SG, as given in Eq. 3, are present across the filtering capacitors shown in Fig. 2. The impedance of the stator windings of the imaginary SG is represented by the inductance L_s and the resistance R_s of the left inductors shown in Fig. 2. Then e_a, e_b, and e_c represent the back EMF due to the movement of the imaginary rotor. The PWM techniques make e_a, e_b, and e_c closely approximate the 3-phase voltages of a real SG. It is assumed that the imaginary field (rotor) winding of the SV is fed by an adjustable dc current source i_f. As long as i_f is constant, the generated voltage from Eq. 4 reduces to

$$e = \theta^{\cdot} M_f\ i_f\ \widetilde{sin}\ \theta \quad (8)$$

The filtering capacitors C should be chosen such that the resonant frequency $1/\sqrt{L_s C}$ is approximately $\sqrt{\omega_n \omega_s}$, where ω_n is the nominal angular frequency of the grid voltage and ω_s is the angular switching frequency used to turn on/off the switches.

B. Electronic Part

Define the generated real power P and reactive power Q (as seen from the inverter legs) as

$$P = \langle i, e\rangle \qquad Q = \langle i, e_q\rangle$$

Where e_q has the same amplitude as e but with a phase delayed from that of e by $\pi/2$, i.e.,

$$e_q = \theta^{\cdot} M_f\ i_f\ \widetilde{sin}(\theta - \pi/2) = -\theta^{\cdot} M_f\ i_f\ \widetilde{cos}\ \theta$$

Then, the real power and reactive power are, respectively

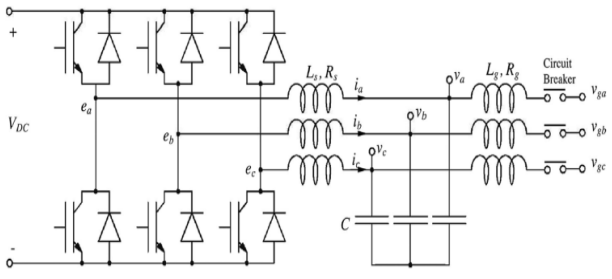

Fig.2. Power parts of a SV

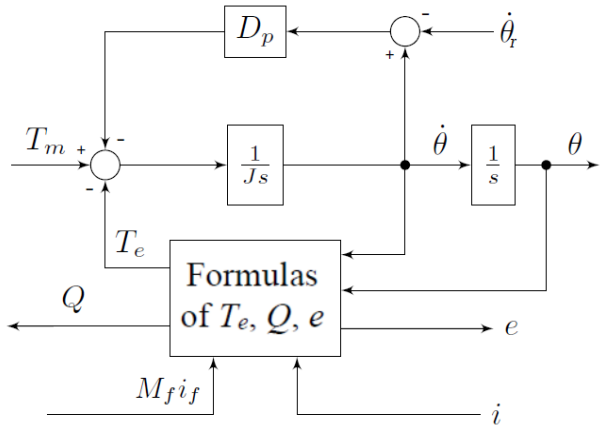

Fig.3. The electronic part of SV

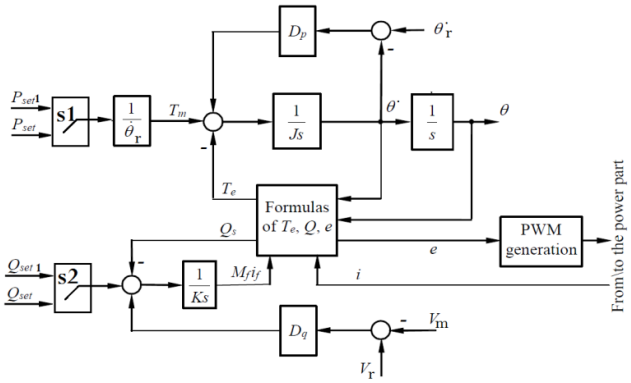

Fig.4. Proposed regulation of the real and reactive power in a synchronverter

$$P = \dot{\theta} M_f\, i_f \langle i, \widetilde{sin}\ \theta \rangle ,$$

$$Q = -\dot{\theta} M_f\, i_f \langle i, \widetilde{cos}\ \theta \rangle \quad (9)$$

These coincide with the conventional definitions for real power and reactive power, usually expressed in *d, q* coordinates. Positive Q corresponds to an inductive load. Note that, if $i = i_0\, \widetilde{sin}\phi$ for some angle ϕ (this would be the case, e.g., in balanced steady-state operation with $\theta - \phi$ constant), then

$$P = \dot{\theta} M_f\, i_f \langle i, \widetilde{sin}\ \theta \rangle = 3/2\ \dot{\theta} M_f\, i_f\, i_0\, cos(\theta - \phi)$$

$$Q = -\dot{\theta} M_f\, i_f \langle i, \widetilde{cos}\ \theta \rangle = 3/2\, \dot{\theta} M_f\, i_f\, i_0 \sin(\theta - \phi)$$

The previous formulas for P and Q are used when regulating the real and reactive power of an SG. "Eq. 6" can be written as

$$\ddot{\theta} = 1/J\ (T_m - T_e - D_p\, \dot{\theta})$$

Where the mechanical torque T_m is a control input while the electromagnetic torque T_e depends on *i* and θ according to Eq. 7. Eq. 7– Eq. 9, are implemented in the electronic part of a SV shown in Fig. 3. Thus, the state variables of the SV are *i* (the inductor currents), *v* (the capacitor voltages), θ, and $\dot{\theta}$ (which are a virtual angle and a virtual angular speed). The control inputs of the SV are T_m and $M_f\, i_f$. In order to operate the SV in a useful way, a controller is needed to generate the signals T_m and $M_f\, i_f$ such that system stability is maintained and the desired values of real and reactive power are followed.

IV. OPERATION OF SYNCHRONVERTER

A. Frequency Drooping and Regulation of Real Power

1) Case of Standalone (island) mode: In this mode SG rotor speed is maintained by the prim-mover and mechanical power of power covers the electrical power developed in addition to all power losses of the power conversion process. As the load increases the speed (and consequently frequency) decreases making speed governor permitting higher fuel input and this brings new power balance at smaller rotor speed (smaller frequency). To bring frequency back to its original value the no-load frequency setting of speed governor need to be raised up. The ratio $D_p = -\Delta T/\Delta\dot{\theta}$.is called the frequency droop. Typical values for the frequency droop are a 100% increase in power for a frequency decrease between 3% and 5% (from nominal values). In Fig. 4 and later, the constant D_p represents the (imaginary) mechanical-friction coefficient plus the frequency-drooping coefficient.

The island mode is implemented in SV as shown in Fig.4 with switch S1 in lower position this is equivalent to $P_{set} = 0, Q_{set} = 0$.

2) Case of Grid connected mode

For SGs, connected with grid the rotor speed is maintained by the grid frequency while the active load share is adjusted by the mechanical power input (P_{set}) from the prime-mover.

An important mechanism for SGs operating in parallel to share load evenly is to vary the real power delivered to the grid according to the SGs individual ratings. This is made by matching the droop characteristics of generators operating in parallel. This is called frequency droop control and is implemented in a SV as shown in Fig. 4 with switch S1 in the upper position. In this case the input (P_{set}) has the dominant effect, and the closed loop control adjust actual power share to be equals to P_{set}.

Because of this built-in frequency-drooping mechanism, a SV automatically shares the load variations with other inverters of the same type and with SGs on the same power grid. The real power regulation loop is very simple because no mechanical devices are involved, and no measurements other than i are needed.

The regulation of the real power shown in the upper part of Fig. 4 has an inner frequency-droop loop (with feedback gain D_p) and the outer real power loop (with the feedback coming from the current i via the torque T_e). The time constant of the frequency-droop loop is $\tau_f = J/D_p$. Hence, if we have decided upon τ_f , then J should be chosen as $J = D_p\tau_f$.

In paper [4] the author used very small J (much smaller than for a real SG) to have fast response in the frequency-droop loop. In our work aiming to make SV having good contribution to power system stored kinetic energy we use value of J very large than that used in [4]. Specifically we used J equals to that of SG with the same power rating. The increased value of time delay τ_f introduced is partially compensated by applying relatively larger value of D_p just to obtain satisfactory transient response. One must make a

compromise between enough inertia contribution and fast dynamic response. However, as will be seen in simulation results the transient response is still faster than a conventional SG.

B. Voltage Drooping and Regulation of Reactive Power

1) Case of Standalone (island) mode: In this mode the terminal voltage is adjusted by excitation field current of SG while the reactive power Q flowing out of the SG equals that of the load. When the load increases the terminal voltage decreases and requires more field current to bring it back to original value.

In this mode there must be a control loop to adjust the terminal voltage to be fixed against load variations. This control loop is known practically as Automatic Voltage Regulator (AVR) and it is very important in SG operation due to the large voltage regulation of this type of generators.

In SV this is realized as shown in the lower part of Fig.4 with switch S2 in the lower position. The difference between the reference voltage V_r and the amplitude V_m of the feedback voltage v_g from Fig. 2 is the voltage amplitude tracking error. This error is multiplied by a gain and used to generate $M_f\, i_f$ similar to main flux in real SG. The reference input Q_{set} in this mode is set to zero.

2) Case of Grid connected mode: In this mode the terminal voltage is fixed by grid. The regulation of reactive power share Q flowing of the SG is adjusted by the field excitation current or excitation emf (E_{max}). Define the voltage drooping coefficient D_q as the ratio of the change of reactive power ΔQ to the change of voltage $\Delta V = E_{max} - V_g$, i.e. $Dq = -\Delta Q \,/\, \Delta V$.

The AVR in this case regulates only the reactive power share of SG; it has no effect on terminal voltage since it is fixed by the grid.

In SV the control loop for the reactive power is realized as shown in the lower part of Fig.4. With the two switches S2 in the upper positions, the difference between the reference value of the reactive power sharing Q_{set} and the actual Q multiplied by the voltage drooping coefficient D_q and is fed into an integrator with a gain $1/K$ to generate $M_f\, i_f$. The reactive power Q is given by Eq. 9.

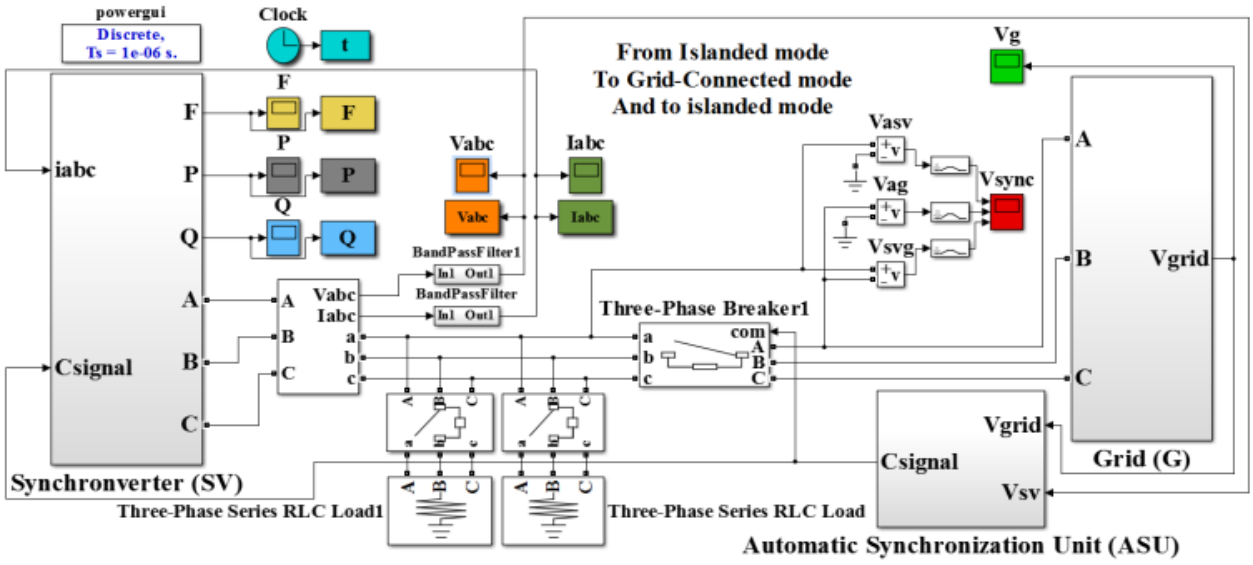

Fig.5 Complete Simulink model of one SV operated in the two modes (Island / Grid)

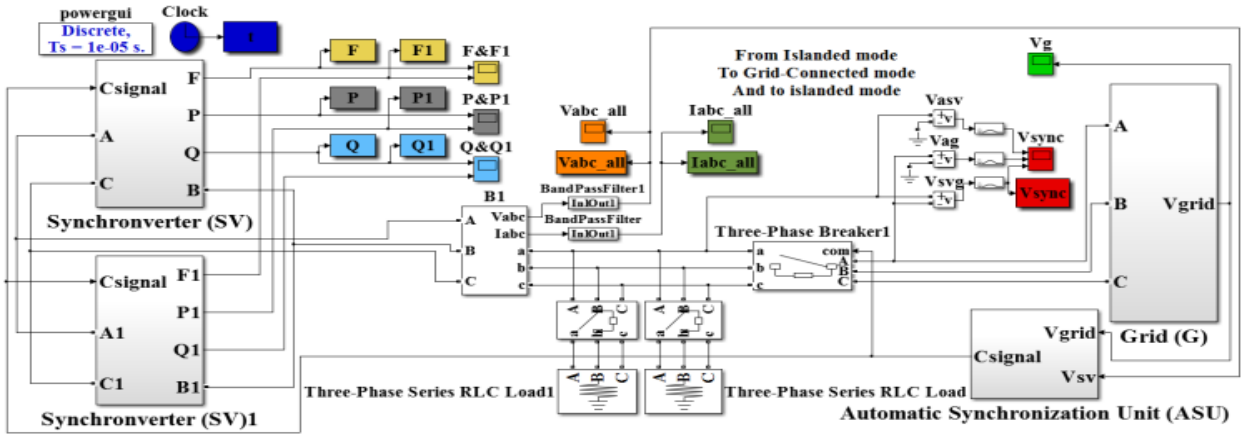

Fig.6 Complete Simulink model of two SVs simulating MG in the two modes (Island / Grid)

The time constant τ_v of the voltage loop can be estimated as; $\tau_v \approx K / \dot{\theta} D_q \approx K / \dot{\theta_r} D_q$.

The variation of $\dot{\theta}$ is very small. Hence, K follows if τ_v and Dq has been chosen. V_m, can be computed as $V_m \approx \dot{\theta} M_f i_f$.

V. SIMULATION AND ANALYSIS OF RESULTS

We use the MATLAB-SIMULINK toolboxes to simulate the complete dynamic model of the SV, with each subsystem model is constructed individually, and then the whole dynamic model is formed by linking the different subsystems together. Important results of some subsystems are presented also in this section. The benefits of simulating the established models are:

- Tuning D_p and τ_f for the selected value of inertia equated to that of the corresponding SG.
- Examining voltage drooping loop in the two modes of operation.
- Studying the conditions of the DC bus under in different conditions.

TABLE I
PARAMETERS OF THE SYNCHRONVERTER AND CONTROLLER

Parameters	Values	Parameters	Values
L_s	5.3 mH	L_g	5.3 mH
R_s	0.166 Ω	R_g	0.166 Ω
C	22 μF	nominal frequency	50 Hz
R(parallel to C)	1000 Ω	nominal voltage (line-line)	220 Vrms
Rated power	16 KVA	DC –link voltage	600 V
Switching Frequency	10 KHz		
J	0.15 Kg.m^2	K	157
Dp	75	Dq	100
τ_f	0.002 s	τv	0.002 s

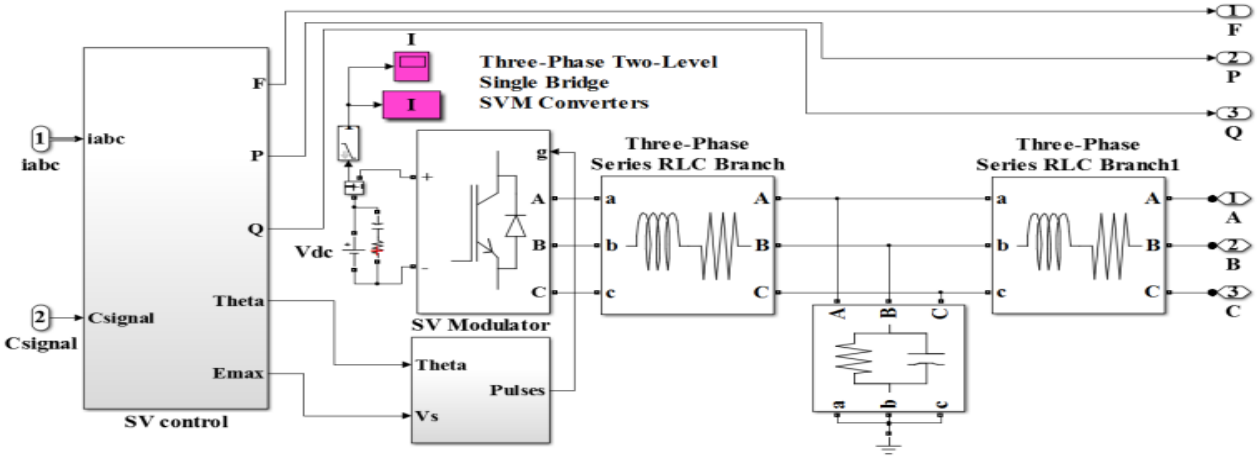

Fig.7 Complete Simulink model of SV

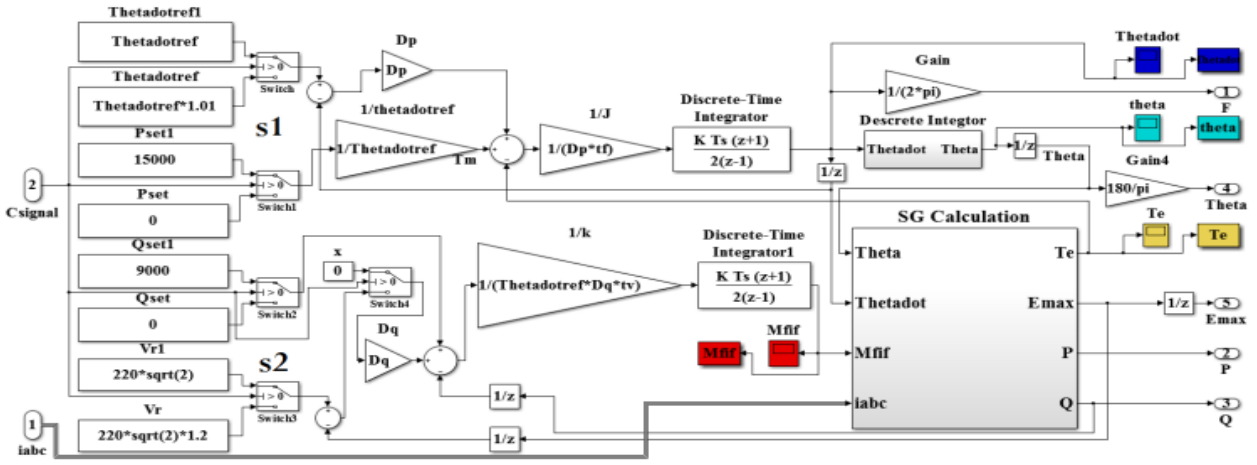

Fig.8 Complete Simulink model of SV control

- Testing the automatic synchronization unit.
- Proving the seamlessly transition between island and grid modes.
- Testing the active and reactive power sharing in MG based on SVs.

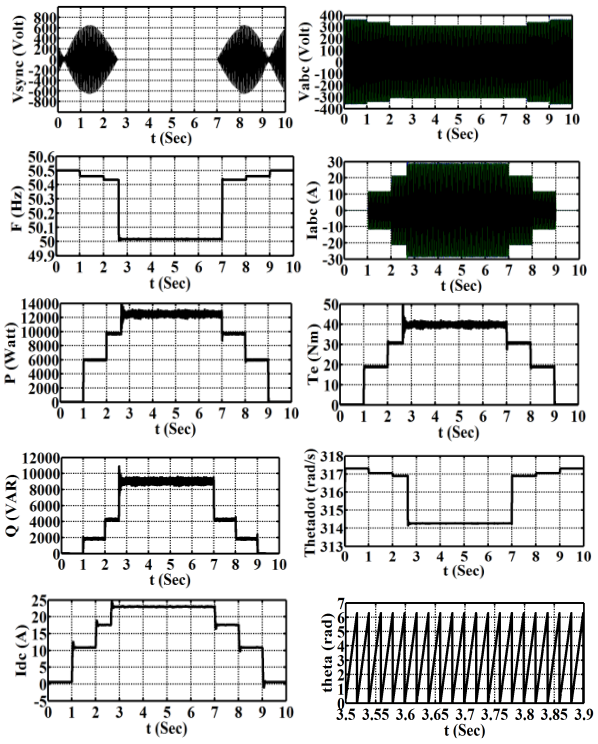

Fig.9. Simulation results of one SV operated in the two modes (Island / Grid)

For the sake of illustration, Fig.5 shows the complete SIMULINK model of one SV operated in the two modes (Island / Grid) and Fig.6 shows the complete SIMULINK model of two SVs simulating MG in the two modes (Island / Grid).

The parameters of the SV and controller used in the simulations are given in Table I. In the following we explain each separate building block and its functions and how it is connected to overall system. Description of building blocks

The SV unit: As shown in Fig.7 containing the SV control unit, PWM inverter unit and low pass filter unit.

A.

1) The SV control unit: Fig.8 gives out the model of the SV in the time domain. It figures out the relationship of the electrical part and the mechanical part. The controller is shown in Fig.8. There are an active power channel and a reactive power channel. The active power channel follows the frequency droop control loop with coefficient D_p as the feedback gain. The reactive power channel uses voltage-droop control loop with the voltage droop coefficient D_q and integral coefficient K. With the controller as core, the SV can regulate the active power and the reactive power independently.

2) PWM Inverter: It is a part of SV control unit applying the Space vector modulation (SVM) technique to generate the switching pulses for the 3-phase inverter bridge according to the required voltage magnitude and phase angle. These are the two outputs of SV control unit.

3) LC filter unit: As shown in Fig.7 the power part of the SV connected to the grid through an LC filter to reduce the voltage and current ripples caused by the high frequency switching of the power devices. The LC filter design is given in section III.

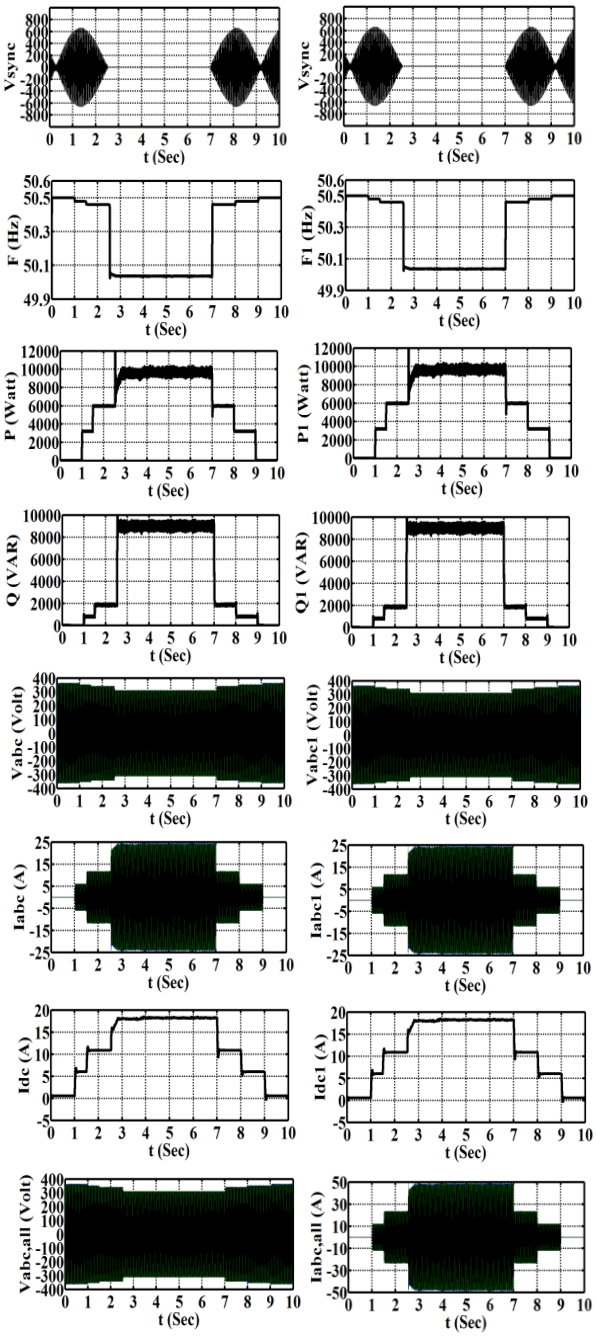

(a) (b)

Fig.10 Simulation results of two SV operating in parallel to simulating MG in the two modes (Island / Grid)

4) Automatic synchronization unit: This unit tests the realization of ideal conditions of synchronization. At the correct instant this unit gives control logic signals to circuit breaker and changeover switches S1 and S2 to select the appropriate configuration of active and reactive power controllers.

5) The Grid unit: As shown in Fig.5 and Fig.6 is simulated by an ideal 3-phase supply standing for infinite bus of fixed voltage and fixed frequency and unlimited capacity.

6) The Loads: As shown in Fig.5 and Fig.6 using three phase series loads by two step.

B. The Simulation Results and Discussions

The SV can feed pre-set real power and reactive power to the grid and can automatically change the real power and reactive power fed to the grid according to the SV input power P_{set} and Q_{set}.

1) One SV operated in the two modes (Island / Grid): As shown in Fig.9 one SV is operated in island mode from t=0 to t=2.65 s, the no-load frequency is set to 50.5 Hz, and a 10kW+4kVAR load is switched on in two steps; at t=1 s and at t=1.5 s. the frequency drops to decreases in proportion to active power loading and the voltage drops in proportion to reactive loading. At t=2.65 s the synchronization unit detects the correct synchronization instant and takes actions to connect SV to grid. In grid mode the active power controller dictates active power share $P_{set} = 15\,kW$ and $Q_{set} = 9\,kVAR$ the SV frequency and voltage drops to their grid values. At t=7 s an intentional islanding is made; circuit breaker is tripped, the P and Q controllers are reconfigured to island operation. The previously connected loads are switched off and finally SV frequency and voltage returns to its no-load value. It worse noticing that the synchronization instant was very accurate. There was no noticeable disturbance caused by this event. The SV responded quickly both to the step change in active and reactive power demand. Concerning the dc link where the voltage is fixed by the battery while the dc current tracks the active power load of SV to satisfy power balance, $Vdc \times Idc = active\ power\ of\ SV$.

2) Two SV operating in parallel to simulate a MG in the two modes (Island / Grid): The MG is operated in sequence of events similar to the previous case. The simulation results are shown in Fig. 10. Generally the results are similar to the previous case with only difference in lies in division of load equally between the two SVs.

VI. CONCLUSION

In this paper, the mathematical model of SV is simulated using Matlab 8.5/Simulink. Detailed simulation blocks are clarified and presented. The model used covers all the dynamics and steady state conditions without the restrictive assumptions normally imposed in such cases. The implementation and operation of SV, including active and reactive load sharing, have been described in detail. The mathematical model used here can be applied to investigate different problems of related to power systems dominated by parallel-operated inverters. In DG the SV is able to transfer seamlessly between the two modes and hence, they provide a solution for smart grid and MGs. An automatic synchronization unit is used to minimize disturbances at instant of connection to grid. Response in different modes of operation is thoroughly examined.

ACKNOWLEDGMENT

I want to thank the source of every success to ALLAH; Next I want to thank my advisors for their guidance and supports throughout the research.

REFERENCES

[1] J. M. Carrasco, L. G. Franquelo, J. T. Bialasiewicz, E. Galvan, R. C. Portillo-Guisado, M. A. M. Prats, J. I. Leon, and N. Moreno-Alfonso, "Power-electronic systems for the grid integration of renewable energy sources: A survey," IEEE Trans. Ind. Electron., vol. 53, no. 4, pp. 1002–1016, Aug. 2006.

[2] M. Prodanovic and T. C. Green, "Control and filter design of three-phase inverters for high power quality grid connection," IEEE Trans. Power Electron., vol. 18, no. 1, pp. 373–380, Jan. 2003.

[3] Z. Ma, Q.-C. Zhong, and J. Yan, "Synchronverter-based control strategies for three-phase pwm rectifiers," in Industrial Electronics and Applications (ICIEA), 2012 7th IEEE Conference on, July 2012, pp. 225–230.

[4] Q.-C. Zhong and G. Weiss, "Synchronverters: Inverters that mimic synchronous generators," Industrial Electronics, IEEE Transactions on, vol. 58, no. 4, pp. 1259–1267, April 2011.

[5] Q.-C. Zhong and T. Hornik, Control of Power Inverters in Renewable Energy and Smart Grid Integration. Wiley-IEEE Press, 2013.

[6] K. De Brabandere, B. Bolsens, J. Van den Keybus, A. Woyte, J. Driesen, and R. Belmans, "A voltage and frequency droop control method for parallel inverters," IEEE Trans. Power Electron., vol. 22, no. 4, pp. 1107– 1115, Jul. 2007.

[7] Q.-C. Zhong, "Robust droop controller for accurate proportional load sharing among inverters operated in parallel," IEEE Trans. Ind. Electron., vol. 60, no. 4, pp. 1281–1290, Apr. 2013.

[8] J. W. Simpson-Porco, F. Dörfler, and F. Bullo, "Synchronization and power sharing for droop-controlled inverters in islanded microgrids," Automatica, vol. 49, no. 9, pp. 2603–2611, 2013.

[9] G. Konstantopoulos, Q.-C. Zhong, B. Ren, and M. Krstic, "Bounded droop controller for parallel operation of inverters," Automatica, vol. 53, pp. 320 – 328, 2015.

[10] J. Liu, Y. Miura, and T. Ise, "Comparison of dynamic characteristics between virtual synchronous generator and droop control in inverter based distributed generators," IEEE Trans. Power Electron., vol. 31, no. 5, pp. 3600–3611, 2016.

[11] J. Alipoor, Y. Miura, and T. Ise, "Power system stabilization using virtual synchronous generator with alternating moment of inertia," IEEE Journal of Emerging and Selected Topics in Power Electronics, vol. 3, no. 2, pp. 451–458, 2015.

[12] P. Piagi and R. H. Lasseter, "Autonomous control of microgrids," in Proc. IEEE Power Eng. Soc. Gen. Meet., 2006.

[13] J. Guerrero, M. Chandorkar, T. Lee, and P. Loh, "Advanced control architectures for intelligent microgrids-Part I: Decentralized and hierarchical control," IEEE Trans. Ind. Electron., vol. 60, no. 4, pp. 1254–1262, Apr. 2013.

[14] H.-P. Beck and R. Hesse, "Virtual synchronous machine," in Proc. 9th Int. Conf. EPQU, 2007, pp. 1–6, 2007.

[15] Q.-C. Zhong and G.Weiss, "Static synchronous generators for distributed generation and renewable energy," in Proc. IEEE PES PSCE,Washington, DC, Mar. 2009, pp. 1–6.

[16] J. Driesen and K. Visscher, "Virtual synchronous generators," in Proc. IEEE Power Energy Soc. Gen. Meeting–Conversion and Delivery of Electrical Energy in the 21st Century, Jul. 2008, pp. 1–3.

[17] T. Shintai, Y. Miura, and T. Ise, "Oscillation damping of a distributed generator using a virtual synchronous generator," Power Delivery, IEEE Transactions on, vol. 29, no. 2, pp. 668–676, 2014.

[18] J. Alipoor, Y. Miura, and T. Ise, "Distributed generation grid integration using virtual synchronous generator with adoptive virtual inertia," in Energy Conversion Congress and Exposition (ECCE), 2013 IEEE, pp. 4546–4552.

[19] S. D'Arco, J. A. Suul, and O. B. Fosso, "A virtual synchronous machine implementation for distributed control of power converters in smartgrids," Electric Power Systems Research, vol. 122, pp. 180–197, 2015.

[20] J. J. Grainger and W. D. Stevenson, Power System Analysis. NewYork: McGraw-Hill, 1994.

[21] A. E. Fitzgerald, C. Kingsley, and S. D. Umans, Electric Machinery. New York: McGraw-Hill, 2003.

[22] P. Kundur, Power System Stability and Control. New York: McGraw-Hill, 1994.

[23] Q.-C. Zhong, P.-L. Nguyen, Z. Ma, and W. Sheng, "Self-synchronized synchronverters: Inverters without a dedicated synchronization unit," Power Electronics, IEEE Transactions on, vol. 29, no. 2, pp. 617–630, Feb 2014.

[24] C.-H. Zhang, Q.-C. Zhong, J.-S. Meng, X. Chen, Q. Huang, S.-H. Chen, and Z.-P. Lv, "An improved synchronverter model and its dynamic behavior comparison with synchronous generator," in Renewable Power Generation Conference (RPG 2013), 2nd IET, Sept 2013, pp. 1–4, 2014.

[25] Z. Ma, Q.-C. Zhong, and J. Yan, "Synchronverter-based control strategies for three-phase PWM rectifiers," in Proc. of the 7th IEEE Conference on Industrial Electronics and Applications (ICIEA), Singapore, Jul. 2012.

[26] Q.-C. Zhong, Z. Ma, W.-L. Ming, and G. C. Konstantopoulos, "Grid friendly wind power systems based on the synchronverter technology," Energy Conversion and Management, vol. 89, no. 0, pp. 719–726, 2015.

[27] Q.-C. Zhong, L. Hobson, and M. G. Jayne, "Classical control of the neutral point in 4-wire 3-phase DC-AC converters," J. Elect. Power Qual. Utilisation, vol. 11, no. 2, pp. 111–119, 2005.

[28] M. Karimi-Ghartemani, "Universal integrated synchronization and control for single-phase dc/ac converters," Power Electronics, IEEE Transactions on, vol. 30, no. 3, pp. 1544–1557, March 2015.

[29] Q.-C. Zhong, Z. Ma, and P.-L. Nguyen, "Pwm-controlled rectifiers without the need of an extra synchronisation unit," in IECON 2012 - 38th Annual Conference on IEEE Industrial Electronics Society, Oct 2012, pp. 691–695.